

Differential neural networks observer for second order systems with sampled and quantized output

Avelar, A., Salgado, I., Ahmed, H., Mera, M. & Chairez, I.

Published PDF deposited in Coventry University's Repository

Original citation:

Avelar, A, Salgado, I, Ahmed, H, Mera, M & Chairez, I 2018, 'Differential neural networks observer for second order systems with sampled and quantized output' IFAC-PapersOnLine, vol 51, no. 3, pp. 490-495.

<https://dx.doi.org/10.1016/j.ifacol.2018.07.327>

DOI 10.1016/j.ifacol.2018.07.327

ESSN 1474-6670

Publisher: Elsevier

Copyright © and Moral Rights are retained by the author(s) and/ or other copyright owners. A copy can be downloaded for personal non-commercial research or study, without prior permission or charge. This item cannot be reproduced or quoted extensively from without first obtaining permission in writing from the copyright holder(s). The content must not be changed in any way or sold commercially in any format or medium without the formal permission of the copyright holders.

Differential neural networks observer for second order systems with sampled and quantized output

A. Avelar, * I. Salgado, ** H. Ahmed, *** M. Mera, ****,† I. Chairez ****

* UPIITA-Instituto Politécnico Nacional, México

** CIDETEC-Instituto Politécnico Nacional, México (email: ijesusr@gmail.com)

*** School of Mechanical, Aerospace and Automotive Engineering, Coventry University, CV1 2TL, UK (email: ac7126@coventry.ac.uk)

**** UPIBI-Instituto Politécnico Nacional, México

† ESIME-Instituto Politécnico Nacional, México

Abstract: Real instrumentation of control systems in digital devices introduces the necessity of considering quantization and sampling information used in the control and estimator design. The aim of this study is designing a state estimator for uncertain second order nonlinear systems based on the approximation enforced by differential neural networks (DNN) with quantized and time-varying sampled output information. The effect of sampling output information is considered as a time-varying delay. The DNN estimates the set of non-linearities in the system structure with the applications of an adaptive approximation. A Lyapunov-Krasovskii functional served to justify the design of the law that adjusted the weights of the DNN. The origin of the estimation error space is practically stable with the approximation enforced by the DNN. Experimental results implement the DNN observer to reconstruct the states of the Van Der Pol Oscillator. The estimation attained with the proposed observer is compared with the results provided by classical linear observer. The evaluation of the least mean square error demonstrates the superior performance of the solution suggested in this study. The Lyapunov-Krasovskii methodology estimates the region of convergence depending on the sampled period and the level of quantization.

© 2018, IFAC (International Federation of Automatic Control) Hosting by Elsevier Ltd. All rights reserved.

Keywords: Second order nonlinear systems, Quantized and sampled output, Differential neural networks, Lyapunov-Krasovskii functional, Learning Laws

1. INTRODUCTION

The effect of sampled and quantized information in the design of state estimators and controllers for nonlinear systems must be considered in real applications, with channel restrictions such as the case of networked processes (Tian et al., 2008). When such control and estimator algorithms are implemented in embedded devices and digital microprocessors (Wakaiki et al., 2017), both the sampling and quantization play a relevant role on the convergence of either the estimation or tracking errors. The main objective of these applications is to avoid the use of personal computers (Brockett and Liberzon, 2000) in the real implementation of control and estimators. When the systems are distant such as the case of networked control systems, the sampling period is considered time-varying and sometimes not bounded.

For linear systems, the design of sampled-data observer design is not difficult due to the simple and exact available discretization of such class of plants (Wang et al., 2017). However, in nonlinear systems, the exact discretization is hardly attainable and its explicit solution is complex. To overcome the problem of sampling in nonlinear systems, many observer design techniques have been proposed and can be categorized into three main directions: approximate discretization (Fu et al., 2017), time-delay conversion, and exact discrete-time design approaches (Bum Koo et al., 2016; Wakaiki et al., 2017).

There exist solutions/models that consider the delay as a potential tool to represent the sampling issue. Recent research considered the concept of Lyapunov-Krasovskii functionals (LKF) instead of the usual Lyapunov functions to deal with the problem of sampled available information with time varying sampled periods (Fridman and Dambrine, 2009).

The application of LKF allows to handle the sampling operated over the continuous-time system. This strategy can be used in designing state estimation and control algorithms despite the presence of discrete-time measurements. Moreover, the solution of a Lyapunov stability analysis allows to estimate the region of convergence for estimation and tracking errors as a function of the quantization level and the maximum delay between two consecutive measures (Poznyak et al., 2011).

The problem of state estimation becomes more difficult when the mathematical description of the work is unavailable or contains uncertainties, perturbations and the output information is corrupted by bounded noises (Bum Koo et al., 2016).

For uncertain or no modelled system dynamics, adaptive techniques have become an attractive tool to design controllers and observers (Li et al., 2017; Folin et al., 2016). Among others, differential neural networks (DNN) are widely used as suitable approximation of uncertain nonlinear systems (Poznyak et al., 2001). Moreover, recent studies deal with the problem of identification of nonlinear signals with delays in the available output.

In this work, a stability analysis proposed a LKF to derive the learning laws and to conclude about the zone of convergence of the estimation error (Alfaro-Ponce et al., 2017).

This manuscript analyses the effect of sampled and quantized output information in the observers design based on DNN for nonlinear second order uncertain systems. The stability analysis employs a Lyapunov-Krasovskii functional and it is capable to obtain an estimation of the zone of convergence for the identification error depending on the level of quantization and the maximal allowed sampling time. Experimental results show the behavior of the DNN observer tested on a Van Der Pol oscillator, which is internally synchronized by a high order sliding modes controller (Ahmed et al., 2018).

2. SECOND ORDER SYSTEMS WITH SAMPLED AND QUANTIZED OUTPUT INFORMATION

2.1 Class of nonlinear systems

Consider the following locally stable second order system (Khalil, 1991) system

$$\dot{x}_1 = x_2, \quad \dot{x}_2 = f(x_1, x_2, t) + g(x_1, x_2)u, \quad \tilde{y} = x_1 + \xi \quad (1)$$

where $x := [x_1 \ x_2]^\top \in \mathcal{D} \subset \mathbb{R}^2$ is the state vector for any time $t \geq 0$ with initial conditions $x_1(0) = x_{1,0}$ and $x_2(0) = x_{2,0}$, $f: \mathbb{R} \times \mathbb{R} \times \mathbb{R}_+ \rightarrow \mathbb{R}$ is a Lipschitz function that describes the dynamics of system (1), $g: \mathbb{R} \times \mathbb{R} \rightarrow \mathbb{R}$ is the function associated to the input signal $u \in \mathbb{R}$. The variable $\tilde{y} \in \mathbb{R}^n$ is the output of the system (1) corrupted by a bounded noise represented by $\xi \in \mathbb{R}$. This paper considers that the system (1) fulfils the following assumptions:

A1. The signal input belongs to the following admissible set

$$U^{Adm} := \{u : |u|^2 \leq u_1 \|x\|^2 + u_2\} \quad (2)$$

with u_1, u_2 being two positive constants. Notice that the admissible control set includes state feedback controllers and even discontinuous controllers like sliding modes. Moreover, the control signal u enforces that the equilibrium point of (1) is stable at least. Therefore the condition $\|x\|^2 \leq x^+$ is valid

A2. The output perturbations ξ are bounded and therefore, they fulfil the next inequality

$$Q_\xi \xi^2 \leq 1, \quad \forall t \geq 0, \quad Q_\xi \in \mathbb{R}^n \quad (3)$$

A3. The available output y is the product of applying the operations of sampling and quantifying over the output \tilde{y} . The variable \bar{y} defines the sampled output of \tilde{y} which satisfies

$$\bar{y} = \sum_{t_k} \tilde{y}(t_k) \chi_{[t_k, t_{k+1})} \quad (4)$$

The function $\chi_{[t_k, t_{k+1})}(\cdot)$ performs the sampling operation over the output \tilde{y} , and it is defined as

$$\chi_{[t_k, t_{k+1})} = \begin{cases} 1 & \text{if } t \in [t_k, t_{k+1}) \\ 0 & \text{otherwise} \end{cases}, \quad k = 0, 1, 2, \dots$$

In consequence, \bar{y} is the piece-wise constant function obtained by sampling and holding the output \tilde{y} at the discrete instants t_k . The actual system output at time t is $y \in \mathbb{R}$ obtained by quantified the sampled signal \bar{y} , that is, $y = \pi(\bar{y})$. Formally, let $Y \subset \mathbb{R}$ be a countable set of all possible values of the output y and the function $\pi: \mathbb{R} \rightarrow Y$

is defined as a projector operator, that is $\pi \circ \pi(\bar{y}) \equiv \pi(\bar{y})$. The image of π is a discrete subset of \mathbb{R} .

A4. The sampling intervals are not regular. However, there exists a maximum sampling interval h defined as

$$h := \max_k (t_k + 1, t_k) \quad (5)$$

A5. The quantization error is bounded, i.e., there exists a positive finite scalar c such that

$$c := \max_{\bar{y} \in \mathbb{R}} |\pi(\bar{y}) - \bar{y}|_{Q_y}^2 \quad (6)$$

where $Q_y \in \mathbb{R}$ is a positive scalar.

According to the assumptions A1-A5, the objective of this paper is to design a state observer for the partially unknown system described in equation (1) considering a sampled and quantized available output such that, the closed-loop trajectories of the estimation error defined as $\Delta = \hat{x} - x$ remains inside a set centered at the origin in spite of the presence of noisy quantized sampled output and uncertainties.

2.2 Neural network representation

The system in (1) can be represented as

$$\begin{aligned} \dot{x}_1 &= x_2, & \dot{x}_2 &= f_0(x, t|\Theta) + \tilde{f}(x, t|\Theta) \\ \tilde{f}(x, t|\Theta) &= f(x_1, x_2, t) + g(x_1, x_2)u - f_0(x, t|\Theta) \end{aligned} \quad (7)$$

where $f_0(x, t|\Theta)$ represents the *nominal dynamics* selected according to designer desires and \tilde{f} is a *vector field* corresponding to the modelling error. We define the parameters $\Theta := [a, w_1^*, w_2^*]$ ($\Theta \in \mathbb{R}^{1 \times (2l+1)}$) that shall be adjusted to enforce the convergence of the DNN to the trajectories of system (1). According to the DNN approach developed in (Poznyak et al., 2001), we define the nominal dynamics as

$$f_0(x, t|\Theta) = ax + w_1^* \sigma(x) + w_2^* \phi(x)u \quad (8)$$

Here, the components of a , namely $a_i \in \mathbb{R}_-$, $w_1^* \in \mathbb{R}^l$ and $w_2 \in \mathbb{R}^l$ are the best fitted values needed to reproduce the dynamics of system (1). $\sigma: \mathbb{R}^2 \rightarrow \mathbb{R}^l$ and $\phi: \mathbb{R}^2 \rightarrow \mathbb{R}^l$ are the activation functions for the DNN structure, that is:

$$\begin{aligned} \sigma_j(x) &:= a_{\sigma_j} \left(1 + b_{\sigma_j} e^{-c_{\sigma_j}^\top x} \right)^{-1} + d_{\sigma_j}, \\ \phi_j(x) &:= a_{\phi_j} \left(1 + b_{\phi_j} e^{-c_{\phi_j}^\top x} \right)^{-1} + d_{\phi_j}, \\ j &= 1, 2, \dots, l \end{aligned} \quad (9)$$

$$a_{\sigma_l}, a_{\phi_l}, b_{\sigma_l}, b_{\phi_l}, d_{\sigma_l}, d_{\phi_l} \in \mathbb{R}, \quad c_{\sigma_l}, c_{\phi_l} \in \mathbb{R}^2$$

All the sigmoid functions considered in this study are continuous and each one of them satisfies the following condition

$$\begin{aligned} \|\sigma(x) - \sigma(x')\| &\leq L_\sigma \|x - x'\| \\ \|\phi(x) - \phi(x')\| &\leq L_\phi \|x - x'\| \end{aligned} \quad (10)$$

where $L_\sigma, L_\phi \in \mathbb{R}_+$. Additionally, by the nature of this class of activation functions, the next condition is also satisfied

$$\|\sigma(x)\| \leq \sigma^+, \quad \|\phi(x)\| \leq \phi^+, \quad \forall x \in \mathcal{D} \quad (11)$$

With $\sigma^+, \phi^+ \in \mathbb{R}_+$. The class of no modelled dynamics are assumed bounded, that is

$$\|\tilde{f}(x, t|\Theta)\|_{\Lambda_f}^2 \leq \tilde{f}^+ \quad (12)$$

where $\tilde{f}^+ \in \mathbb{R}_+$. In general, the weights w_i^* ($i = 1, 2$) are unknown. However, they are bounded as

$$(w_i^*)^\top \Lambda_{w_i}^{-1} w_i^* \leq \bar{w}_i \quad (13)$$

$\Lambda_{w_i} \in \mathbb{R}^{n \times n}$ is a known positive definite and symmetric matrix and $\bar{W}_i \in \mathbb{R}^{n \times n}$ is a given matrix.

2.3 Problem formulation

The problem considered in this paper is to design an asymptotic observer that generates the estimates \hat{x} based on the measure of the state y with quantized and sampled output information. The design includes the development of adaptive learning laws for the adaptive based DNN observer. The main goal is to fulfil the following condition

$$\lim_{t \rightarrow \infty} \|\hat{x} - x\| \leq \varepsilon_{\bar{x}}, \quad \varepsilon_{\bar{x}} \in \mathbb{R}_+ \quad (14)$$

3. DIFFERENTIAL NEURAL NETWORK OBSERVER WITH SAMPLED AND QUANTIZED OUTPUT

3.1 DNN Observer

Following the solution proposed in (Poznyak et al., 2001), the DNN identifier satisfies the following structure

$$\dot{\hat{x}} = A\hat{x} + W_1 \sigma(\hat{x}) + W_2 \phi(\hat{x})u + L(\hat{y} - y), \quad \hat{y} = C\hat{x} \quad (15)$$

with initial condition $\hat{x}(0) = \hat{x}_0 \in \mathbb{R}^2$ and the following parameters

$$A = \begin{bmatrix} 0 & 1 \\ \rho & a \end{bmatrix}, \quad W_i = M w_i, \quad M = [0 \ 1]^\top, \quad \rho \in \mathbb{R}_- \quad (16)$$

Special updating (learning) laws $\dot{W}_i = \Phi(W_i, \hat{x})$ actualize the values of the free parameters of system (15).

3.2 Learning laws for the DNN observer

Let define the output error as $e = \hat{y} - y$. Then, the adaptive learning laws $\Phi_i(W_i, \hat{x}|W_i^*)$ for the free parameters W_i with $i = [1, 2]$ is given by (the procedure to obtain the learning law is given in the proof of Theorem 1)

$$\begin{aligned} \dot{W}_i &= -\alpha \tilde{W}_i - k_i^{-1} P N_\mu^\top \Psi_i e^\top C^\top - \\ &\quad \mu k_i^{-1} P (\tilde{\Lambda}_{\Psi_i} + Q_{W_i}) P \tilde{W}_i \Psi_i^\top, \\ i &= [1, 2], \quad \Psi_1 = \sigma(\hat{x}), \quad \Psi_2 = \phi(\hat{x})u \end{aligned} \quad (17)$$

Here, $0 < Q_{W_i} = Q_{W_i}^\top \in \mathbb{R}^{2 \times 2}$ and $0 < \tilde{\Lambda}_{\Psi_i} = \tilde{\Lambda}_{\Psi_i}^\top \in \mathbb{R}^{2 \times 2}$. In the last equation, $W_i(0) = W_i^o$ are the known initial conditions for the weights. The terms k_i are the learning coefficient of the DNN observer and P is the solution of the matrix inequality (18):

$$\Omega := \begin{bmatrix} \omega_1 & \omega_2^\top & 0 & -P & PLC & 0 & 0 \\ \omega_2 & -2P & 0 & -P & PLC & P & P \\ 0 & 0 & -h^{-\alpha h} S & 0 & 0 & 0 & 0 \\ -P & -P & 0 & -Q_{\tilde{f}} & 0 & 0 & 0 \\ PLC & PLC & 0 & 0 & -Q_y & 0 & 0 \\ 0 & P & 0 & 0 & 0 & -Q_{W_i} & 0 \\ 0 & P & 0 & 0 & 0 & 0 & -Q_{W_2} \end{bmatrix} \quad (18)$$

$$\omega_1 := PA + A^\top P + PLC + C^\top L^\top P + PRP + Q,$$

$$\omega_2 := PA + PLC$$

With the following parameters

$$\begin{aligned} Q &:= N_\mu^\top (\Lambda_{\Psi_1}^{-1} + \Lambda_{\Psi_2}^{-1}) N_\mu, \quad R = \Lambda_{W_1} + \Lambda_{W_2}, \\ N_\mu &= (\mu I_{n \times n} + CC^\top)^{-1} \end{aligned} \quad (19)$$

and S , Q_y , $W_{\tilde{f}}$, Q_{W_1} and Q_{W_2} being positive definite matrices with dimension 2×2 .

3.3 Estimation result

The following Lemma is used to develop the stability proof:

Lemma 1. (Jensen's inequality)(Poznyak et al., 2011) For any matrix $\mathbb{R}^{n \times n}$, scalar $h > 0$ and a vector function $\phi : [-h, 0] \rightarrow \mathbb{R}^n$ such that the integrations concerned are well defined, the following holds

$$\int_{-h}^0 \phi(s)^\top R \phi(s) ds \geq \frac{1}{h} \int_{-h}^0 \phi^\top(s) ds R \int_{-h}^0 \phi(s) ds$$

The next theorem summarizes the theoretical result for the state and input identification

Theorem 1. Consider the nonlinear system defined in equation (1) and the DNN observer defined in (15) together with the learning laws in (17). If the matrix inequality defined in (18) is feasible for a positive definite solution $P = P^\top > 0$, then, the equilibrium point of the estimation error e is practically stable with an ultimate invariant set Ξ centered on the origin and defined as

$$\Xi := \frac{\beta}{\alpha}, \quad \beta := 1 + (W_i^o)^\top \Psi_i^+ + f^+ + c, \quad \alpha \in \mathbb{R}_+ \quad (20)$$

Proof 1. Consider the following LKF

$$\begin{aligned} V(\Delta, \dot{\Delta}, W_i) &= \Delta^\top P \Delta + k_i \text{tr} \left\{ \tilde{W}_i^\top \tilde{W}_i \right\} + \\ &\quad h \int_{\theta=-h}^0 \int_{s=t+\theta}^t e^{\alpha(s-t)} \dot{\Delta}^\top(s) S \dot{\Delta}(s) ds d\theta \end{aligned} \quad (21)$$

With $i = 1, 2$. The estimation error is defined as $\Delta := \hat{x} - x$. The time derivative of the functional (21) is the following

$$\begin{aligned} \dot{V}(t) &= 2\Delta^\top P \dot{\Delta} - \alpha h \int_{-h}^0 \int_{t+\theta}^t e^{\alpha(s-t)} \dot{\Delta}^\top(s) S \dot{\Delta}(s) ds d\theta - \\ &\quad h \int_{t-h}^t e^{\alpha(s-t)} \dot{\Delta}^\top(s) S \dot{\Delta}(s) ds + h^2 \dot{\Delta}^\top(t) S \dot{\Delta}(t) + \\ &\quad 2\text{tr} \left\{ \dot{\tilde{W}}_i^\top \tilde{W}_i \right\} \end{aligned} \quad (22)$$

The dynamics of the estimation error are defined as

$$\begin{aligned} \dot{\Delta} &= A\Delta + \tilde{W}_1 \sigma(\hat{x}) + \tilde{W}_2(t) \phi(\hat{x})u + (W_1^*)^\top \tilde{\sigma} + \\ &\quad (W_2^*)^\top \tilde{\phi}u + L(\hat{y} - y) - \tilde{f} \end{aligned} \quad (23)$$

In equation (23) \tilde{f} is the simplified notation for $\tilde{f}(x, t|\theta)$. Let apply the method proposed by (Fridman and Dambrine, 2009) known as the Descriptor method which consist of adding the following null term

$$\begin{aligned} \tilde{\mathcal{D}}(\Delta, \dot{\Delta}) &:= \left(2\Delta^\top P + 2\dot{\Delta}^\top P \right) (A\Delta + \tilde{W}_1 \sigma(\hat{x}) + \tilde{W}_2(t) \phi(\hat{x})u) + \\ &\quad \left(2\Delta^\top P + 2\dot{\Delta}^\top P \right) \left((W_1^*)^\top \tilde{\sigma} + (W_2^*)^\top \tilde{\phi}u \right) + \\ &\quad \left(2\Delta^\top P + 2\dot{\Delta}^\top P \right) (L(\hat{y} - y) - \tilde{f} - \dot{\Delta}) \end{aligned} \quad (24)$$

To introduce the effect of the quantized and sampled output let add and subtract the term \tilde{y} into the descriptor term

$$\begin{aligned} \mathcal{D}(\Delta, \dot{\Delta}) = & \left(2\Delta^\top P + 2\dot{\Delta}^\top P \right) (A\Delta + \tilde{W}_1 \sigma(\hat{x}) + \tilde{W}_2(t)\phi(\hat{x})u) + \\ & \left(2\Delta^\top P + 2\dot{\Delta}^\top P \right) \left((W_1^*)^\top \tilde{\sigma} + (W_2^*)^\top \tilde{\phi}u \right) + \\ & \left(2\Delta^\top P + 2\dot{\Delta}^\top P \right) (LC\Delta + LC\delta y - \tilde{f} - \dot{\Delta}) \end{aligned} \quad (25)$$

In equation (25), the term $LC\delta y$ represents the difference between the real available output and the output without being sampled and quantized as it was described in assumption A5. Based on this result, and the addition of the term $\alpha V - \alpha V$, the equation (22) is transformed into

$$\begin{aligned} \dot{V}(t) \leq & -\alpha V + 2\Delta^\top P\dot{\Delta} + \Delta^\top P\Delta + \alpha k_i \left\{ \tilde{W}_i^\top \tilde{W}_i \right\} - \\ & h \int_{t-h}^t e^{\alpha(s-t)} \dot{\Delta}^\top(s) S \dot{\Delta}(s) ds + h^2 \dot{\Delta}^\top(s) S \dot{\Delta}(s) + \\ & + 2k_i \left\{ \tilde{W}_i^\top \dot{W}_i \right\} + \left(2\Delta^\top P x + 2\dot{\Delta}^\top P \right) (-\tilde{f} - \dot{\Delta}) + \\ & \left(2\Delta^\top P x + 2\dot{\Delta}^\top P \right) (A\Delta + \tilde{W}_1 \sigma(\hat{x}) + \tilde{W}_2(t)\phi(\hat{x})u) + \\ & \left(2\Delta^\top P x + 2\dot{\Delta}^\top P \right) \left((W_1^*)^\top \tilde{\sigma} + (W_2^*)^\top \tilde{\phi}u \right) + \\ & \left(2\Delta^\top P x + 2\dot{\Delta}^\top P \right) (LC\Delta + LC\delta y) \end{aligned}$$

By the Lemma 1 the term $h \int_{t-h}^t e^{\alpha(s-t)} \dot{\Delta}^\top(s) S \dot{\Delta}(s) ds$ becomes:

$$-h \int_{t-h}^t e^{\alpha(s-t)} \dot{\Delta}^\top(s) S \dot{\Delta}(s) ds \leq -he^{\alpha h} \int_{t_k}^t \dot{\Delta}^\top(s) S \int_{t_k}^t \dot{\Delta}(s)$$

Defining the extended state vector η as

$$\eta := \begin{bmatrix} \Delta^\top & \dot{\Delta}^\top & \left(\int_{t_k}^t \dot{\Delta}(s) ds \right)^\top & \tilde{f}^\top & \delta y^\top & (W_1^*)^\top & (W_2^*)^\top \phi u \\ \Delta^\top & \dot{\Delta}^\top & (\Delta(t) - \Delta(t_k))^\top & \tilde{f}^\top & \delta y^\top & (W_1^*)^\top & (W_2^*)^\top \phi u \end{bmatrix} =$$

Equation (22) becomes into

$$\begin{aligned} \dot{V} = & -\alpha V + \alpha k_i \left\{ \tilde{W}_i^\top \tilde{W}_i \right\} + 2k_i \left\{ \tilde{W}_i^\top \dot{W}_i \right\} + \\ & \eta^\top \Omega_1 \eta + 2\Delta^\top P \tilde{W}_1 \sigma(\hat{x}) + 2\Delta^\top P \tilde{W}_2 \phi(\hat{x})u + \\ & 2\Delta^\top P W_1^* \tilde{\sigma} + 2\dot{\Delta}^\top P W_1^* \tilde{\sigma} + 2\dot{\Delta}^\top P W_2^* \tilde{\phi}u W_2^* \tilde{\phi}u \end{aligned} \quad (26)$$

With Ω_1 defined as

$$\Omega_1 := \begin{bmatrix} \omega_{11} & \omega_{12} & 0 & -P & PLC & 0 & 0 \\ \omega_{12}^\top & -2P & 0 & -P & PLC & P & P \\ 0 & 0 & -h^{-\alpha h} S & 0 & 0 & 0 & 0 \\ -P & -P & 0 & 0 & 0 & 0 & 0 \\ PLC & PLC & 0 & 0 & 0 & 0 & 0 \\ 0 & P & 0 & 0 & 0 & 0 & 0 \\ 0 & P & 0 & 0 & 0 & 0 & 0 \end{bmatrix} \quad (27)$$

$$\omega_{11} = PA + A^\top P + PLC + C^\top L^\top P$$

$$\omega_{12} = A^\top P + C^\top L^\top P$$

To introduce the output error $e(t) := \hat{y} - y$ in the Lyapunov analysis, let us apply the following identity

$$\Delta = N_\mu C e + \mu N_\mu \Delta + N_\mu C \xi \quad (28)$$

With μ a small number and N_μ defined in (19). Then, the term $2\Delta^\top P \tilde{W}_1 \sigma(\hat{x})$ turns into:

$$\begin{aligned} 2\Delta^\top P \tilde{W}_1 \sigma(\hat{x}) = & 2e^\top C^\top N_\mu P \tilde{W}_1 \sigma(\hat{x}) + \mu \Delta^\top N_\mu^\top P \tilde{W}_1 \sigma(\hat{x}) + \\ & \xi^\top C^\top N_\mu^\top P \tilde{W}_1 \sigma(\hat{x}) \end{aligned} \quad (29)$$

Assume that we may consider an off-line training that gives an approximation of W_i^* . With an appropriate training, it is possible to define $\tilde{W}_i = W_i - W_i^o$. Where W_i^o are the weights obtained from the off-line training algorithm. Adding and subtracting the term $2\Delta^\top P W_i^o \sigma(\hat{x})$, equation (29) becomes into

$$\begin{aligned} 2\Delta^\top P \tilde{W}_1 \sigma(\hat{x}) = & 2e^\top C^\top N_\mu P \tilde{W}_1 \sigma(\hat{x}) + \mu \Delta^\top N_\mu^\top P \tilde{W}_1 \sigma(\hat{x}) + \\ & \xi^\top C^\top N_\mu^\top P \tilde{W}_1 \sigma(\hat{x}) + 2\Delta^\top P (W_1^o - W_1^*) \sigma(\hat{x}) \end{aligned} \quad (30)$$

With the same arguments $2\Delta^\top P \tilde{W}_2 \phi(\hat{x})u$ is described by

$$\begin{aligned} 2\Delta^\top P \tilde{W}_2 \phi(\hat{x})u = & 2e^\top C^\top N_\mu P \tilde{W}_2 \phi(\hat{x})u + \mu \Delta^\top N_\mu^\top P \tilde{W}_2 \phi(\hat{x})u + \\ & \xi^\top C^\top N_\mu^\top P \tilde{W}_2 \phi(\hat{x})u + 2\Delta^\top P (W_2^o - W_2^*) \phi(\hat{x})u \end{aligned} \quad (31)$$

Based on the definition of Ψ_1 and Ψ_2 as in equation (17) and considering the application of the inequality

$$\begin{aligned} X^\top Y + \left(X^\top Y \right)^\top & \leq X^\top \Lambda^{-1} X + Y^\top \Lambda Y, \\ X, Y \in \mathbb{R}^{p \times s}, \quad & \Lambda \in \mathbb{R}^{s \times s} \end{aligned} \quad (32)$$

The next result is obtained using the inequality given in (32) a number of times

$$\begin{aligned} \dot{V} \leq & -\alpha V + \alpha k_i \left\{ \tilde{W}_i^\top \tilde{W}_i \right\} + 2k_i \left\{ \tilde{W}_i^\top \dot{W}_i \right\} + \eta^\top \Omega_2 \eta + \\ & 2e^\top C^\top N_\mu P W_i \Psi_i + \mu \Psi_i^\top \tilde{W}_i P \tilde{\Lambda}_\Psi P \tilde{W}_i \Psi_i + \\ & + \xi^\top \Lambda_\Psi^{-1} \xi + \Psi_i^\top (W_i^o - W_1^*)^\top \Lambda_W^{-1} (W_i^o - W_1^*) \Psi_i \end{aligned} \quad (33)$$

where $\tilde{\Lambda}_\Psi = \Lambda_\Psi + N_\mu C \Lambda_\Psi C^\top N_\mu^\top$ and $\Omega_2 = \Omega_1 + \mathbf{diag} \{ N_\mu^\top \Lambda_\Psi^{-1} N_\mu + P \Lambda_W P, 0, 0, 0, 0, 0, 0 \}$. Notice that, by assumption A1 the selection $\Lambda_\phi = Q_\xi$, $\xi^\top Q_\xi \xi \leq 1$ and $\|(W_i^o - W_1^*) \Psi_i\|_{\Lambda_W^{-1}}^2 \leq (W_i^o)^\top \Psi_i^+$. Adding and subtracting the terms $\|\tilde{f}\|_{Q_f}^2$, $\|\Delta y\|_{Q_y}^2$, $\|\tilde{W}_i \Psi_i\|_{Q_{W_i}}^2$ equation (34) turns into

$$\begin{aligned} \dot{V} \leq & -\alpha V + \alpha k_i \left\{ \tilde{W}_i^\top \tilde{W}_i \right\} + 2k_i \left\{ \tilde{W}_i^\top \dot{W}_i \right\} + \eta^\top \Omega \eta + \\ & 2e^\top C^\top N_\mu P W_i \Psi_i + \mu \Psi_i^\top \tilde{W}_i P \tilde{\Lambda}_\Psi P \tilde{W}_i \Psi_i + \\ & 1 + (W_i^o)^\top \Psi_i^+ + \|\tilde{f}\|_{Q_f}^2 + \|\Delta y\|_{Q_y}^2 + \|\tilde{W}_i \Psi_i\|_{Q_{W_i}}^2 \end{aligned} \quad (34)$$

where $\Omega := \Omega_2 + \mathbf{diag} \{ 0, 0, 0, -Q_f, -Q_y, -Q_{W_1}, -Q_{W_2} \}$. Considering that for any two vectors $r_1, r_2 \in \mathbb{R}^n$ and a matrix $A \in \mathbb{R}^{n \times n}$, the identity $r_1^\top A r_2 = \mathbf{tr}(r_1^\top A r_2) = \mathbf{tr}(A r_1^\top r_2)$ holds, the simplified version of inequality (34) is

$$\dot{V} \leq -\alpha V + \beta + k_i \left\{ \tilde{W}_i^\top L_{W_i} \right\} + \eta^\top \Omega \eta \quad (35)$$

where β is given by $\beta := 1 + (W_i^o)^\top \Psi_i^+ f^+ + c$,

and L_{W_i} by

$$L_{W_i} = k_i \dot{W}_i + \alpha k_i \tilde{W}_i + P N_\mu^\top \Psi_i e^\top C^\top + \mu P (\tilde{\Lambda}_\Psi + Q_{W_i}) P \tilde{W}_i \Psi_i \Psi_i^\top$$

Lets consider that $L_{W_i} = 0$ (based on the learning laws that adjust the weights), if the feasible matrix $P = P^\top$ solution of the matrix inequality $\Omega \leq 0$, then, the inequality (35) turns into $\dot{V} \leq -\alpha V + \beta$. By the comparison principle Khalil (1991) one finally obtains

$$V(t) \leq e^{-\alpha t} V(0) + \frac{\beta}{\alpha} (1 - e^{-\alpha t}) \quad (36)$$

Based on the previous result, the following upper limit $\lim_{t \rightarrow \infty} V(t) = \frac{\beta}{\alpha}$ finalizes the proof.

4. EXPERIMENTAL RESULTS

To illustrate the estimation performance of the DNN observer under the operations of sampled and quantized output, let us consider the Van Der Pol Oscillator given by the following set of differential equations

$$\dot{x}_1 = x_2, \quad \dot{x}_2 = -x_1 + \kappa(1 - x_1^2) + u, \quad y = x_1 \quad (37)$$

where κ is the model parameter equal to 0.1. Figure 1 shows the electronic circuit and the computer interface. The circuit parameters can be found in (Ahmed et al., 2018). The computer interface employs a dSPACE 1104 board. The Van Der Pol oscillator is internally controlled by a Continuous Singular Terminal Sliding-Mode (CSTSM) controller given by

$$\begin{aligned} \phi &= x_2 - \dot{y}_d + k_2[x_1 - y_d]^{\frac{2}{3}} \\ u &= \ddot{y}_d + x_1 - \kappa x_2(1 - x_1^2) - k_1[\phi]^{\frac{1}{2}} + z \\ \dot{z} &= -k_3[\phi]^0 \end{aligned} \quad (38)$$

where y_d is the desired trajectory to follow, z is an extended variable, $k_1 = 4, k_2 = 3$ and $k_3 = 2$ are design parameters. The dSPACE board runs at 5KH and the controller was implemented with an Euler integration method.

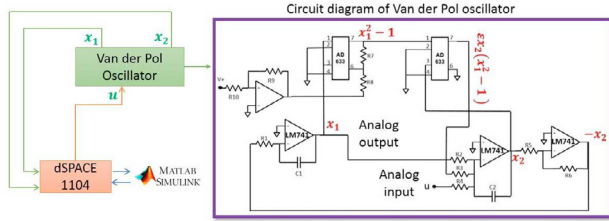


Fig. 1. Schematic overview of the practical implementation and circuit diagram of an autonomous Van Der Pol oscillator.

The DNN observer was implemented with different sampling times and quantization values to compare its performance. The sampling times selected for comparison purposes were 0.0018 and 0.018 seconds. The levels of quantization were chosen as 0.0001, 0.001 and 0.05. These values were chosen to show a significant effect of the operations of sampling and quantization in the experimental results. Moreover, a classical linear observer with the following structure was proposed as $\hat{x}_{1,L} = \hat{x}_{2,L} + G_1(\hat{y} - y)$ and $\hat{x}_{2,L} = G_2(\hat{y} - y)$. The estimates of the states obtained by this observer are compared with the performance of the DNN observer, where $G_1 = -20$ and $G_2 = -55$ are the gains of the observer. The values used in the activation functions in the DNN observer were

$$\begin{aligned} a_{\sigma_1} &= 40, & b_{\sigma_1} &= 1, & c_{\sigma_1} &= \begin{bmatrix} 0.5 \\ 0.5 \end{bmatrix}, & d_{\sigma_1} &= -0.5, \\ a_{\sigma_2} &= 12, & b_{\sigma_2} &= 1, & c_{\sigma_2} &= \begin{bmatrix} 25 \\ 25 \end{bmatrix}, & d_{\sigma_2} &= -0.5, \\ a_{\phi_1} &= 10, & b_{\phi_1} &= 1, & c_{\phi_1} &= \begin{bmatrix} 0.2 \\ 0.7 \end{bmatrix}, & d_{\phi_1} &= -0.65, \\ a_{\phi_2} &= 15, & b_{\phi_2} &= 1, & c_{\phi_2} &= \begin{bmatrix} 12.3 \\ 12.3 \end{bmatrix}, & d_{\phi_2} &= -0.1, \end{aligned}$$

The matrices A and P were selected as

$$A = \begin{bmatrix} 0 & 1 \\ -0.01 & -1000 \end{bmatrix}, \quad P = \begin{bmatrix} 60 & 40 \\ 40 & 106 \end{bmatrix}$$

The learning coefficients are chosen as $k_1 = k_2 = 0.8$ and $\alpha = 0.01, \mu = 0.5, \tilde{L}\Psi_1 = QW_i = I_{2 \times 2}$ and $L = [12.5 \ 10.9]^T$. Figure 2 shows the state estimation of the Van Der Pol oscillator for different sampling times and levels of quantization, with the values of $\tau = 0.00018$ and $q = 0.0001$, the DNN observer estimates the unmeasurable states with better precision than the linear observer.

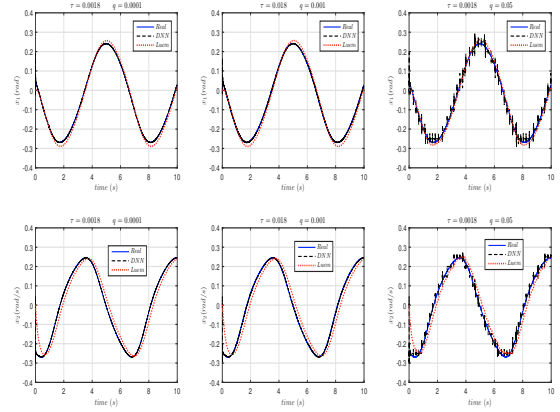


Fig. 2. State estimation of the Van Der Pol states by means of DNN and Luenberger observer at different sampled times and quantization levels. The blue continuous line is the real experimental measurement, the dashed black line is the estimation provided by the DNN. The dotted red line is the linear response obtained with a classical Luenberger observer with unknowledge of the mathematical description.

The DNN reconstructs the states after a small period of learning time smaller than the time of 0.1 seconds. The value of matrix P allows to have a faster adaptation. When the sampling period and the quantization levels are augmented by 10 times, the evolution of time of the DNN observer and the linear observer exhibit almost a similar behavior that in the previous case. However, there exists oscillations with larger amplitudes in the state estimation process with these values. This is evident when the Euclidean norm of the estimation error is plotted.

Figure 3 shows the performance index (Euclidean norm) of each observer at different sampling time and levels of quantization. The second graph shows oscillations with larger oscillations as a consequence of the increment in the sampling period as it was described before. Based on a sampling period $\tau = 0.0018$ and quantization level of $q = 0.05$, the estimation of the unmeasured states by the DNN presents oscillations of a very large oscillations at each measured output. At the first sight, it seems that the linear observer has better performance. However, is one considers a closer view (see figure 4), the state estimation process with the DNN observer shows oscillations with large values around the real trajectories.

Figure 4 also presents the output used in the training of the DNN. Notice, that the DNN adapts its trajectories to the particular square shape (consequence of the sampled and quantized output) in the available output. The linear observer has permanent steady state error. The experimentation shows a better estimation when the DNN is applied.

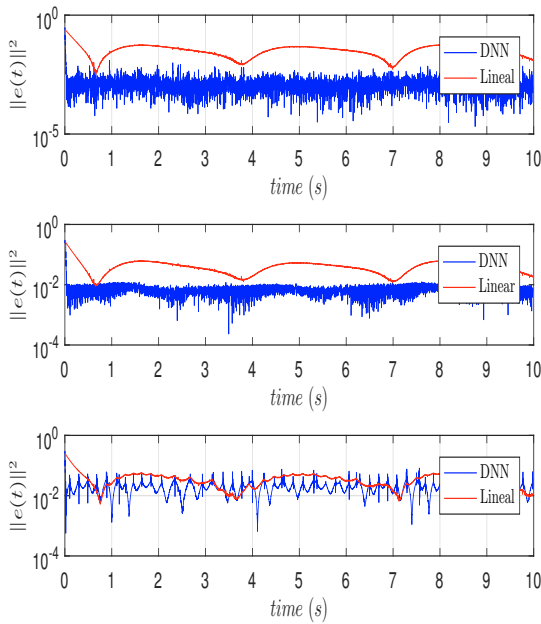


Fig. 3. Euclidean norm of the estimation error for different sampled times and quantization levels. The effect of sampling is clearly evidenced in the oscillations of the estimated states. The upper bound of oscillations is estimated by the stability analysis developed in this study.

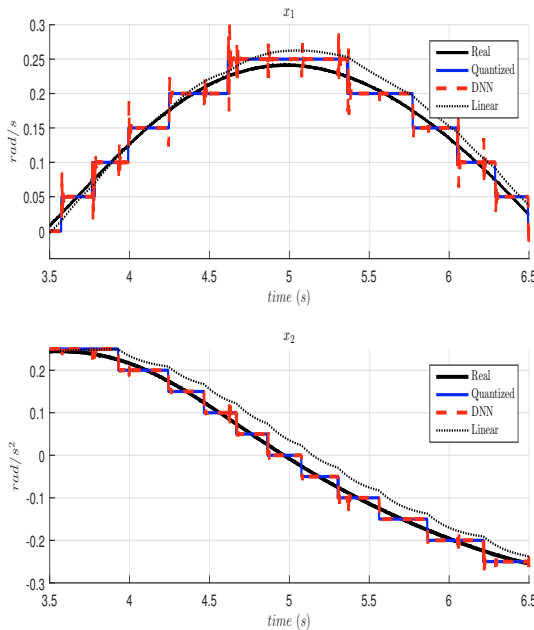


Fig. 4. Closer view to the state estimation process with sampled period $\tau = 0.0018$ and quantization level $q = 0.05$. This graph includes the available output used in the estimation process. Notice that DNN is slightly affected by the sampling process but still its trajectories follow the sampled states evolution.

5. CONCLUSIONS

This manuscript presents the analysis of a DNN observer under the operations of sampled and quantized output. The stability

analysis by LKF allows to define the zone of convergence for the estimation error dependent of the maximal sampled time and the admissible value of quantization. This analysis is crucial in real implementations, when the observers and possible control designs are embedded in digital processors and the problems of digital quantization becomes a problem. Further research has to be oriented in the design of controllers based on the estimated states and the applications of optimization procedures to reduce the zone of convergence for the estimation error.

REFERENCES

- Ahmed, H., Salgado, I., and Ríos, H. (2018). Robust synchronization of master-slave chaotic systems using approximate model: An experimental study. *ISA transactions*. doi: <https://doi.org/10.1016/j.isatra.2018.01.009>.
- Alfaro-Ponce, M., Argüelles, A., and Chairez, I. (2017). Windowed electroencephalographic signal classifier based on continuous neural networks with delays in the input. *Expert Systems with Applications*, 68, 1 – 10. doi: [10.1016/j.eswa.2016.08.020](https://doi.org/10.1016/j.eswa.2016.08.020).
- Brockett, R. and Liberzon, D. (2000). Quantized feedback stabilization of linear systems. *IEEE Transactions on Automatic Control*, 45(7), 1279–1289.
- Bum Koo, G., Bae Park, J., and Hoon Joo, Y. (2016). Decentralized sampled-data fuzzy observer design for nonlinear interconnected systems. *IEEE Trans. on Fuzzy Systems*, 24(3). doi: [10.1109/TFUZZ.2015.2470564](https://doi.org/10.1109/TFUZZ.2015.2470564).
- Folin, T., Ahmed-Ali, T., Giri, F., Burlion, L., and Lamnabhi-Lagarrique, F. (2016). Sampled-data adaptive observer for a class of state-affine output-injection nonlinear systems. *IEEE Trans. on Aut. Ctrl.*, 61(2), 462–467.
- Fridman, E. and Dambrine, M. (2009). Control under quantization saturation and delay: An LMI approach. *Automatica*, 45(10), 2258–2264. doi: [j.automatica.2009.05.020](https://doi.org/10.1016/j.automatica.2009.05.020).
- Fu, X., Kang, Y., and Li, P. (2017). Sampled-data observer design for a class of stochastic nonlinear systems based on the approximate discrete-time models. *IEEE/CAA journal of automatica sinica*, 4(3), 507–511.
- Khalil, H. (1991). *Nonlinear Systems*. Prentice Hall, Upper Saddle River, NJ.
- Li, H., Bai, L., Wang, L., Zhou, Q., and Wang, H. (2017). Adaptive neural control of uncertain nonstrict-feedback stochastic nonlinear systems with output constraint and unknown dead zone. *IEEE Transactions on Systems, Man, and Cybernetics: Systems*, 47(8), 2048–2059.
- Poznyak, A., Sanchez, E., and Yu, W. (2001). *Differential Neural Networks for robust nonlinear control*. World Scientific Publishing Co. Pre. Ltd.
- Poznyak, A., Azhmyakov, V., and Mera, M. (2011). Practical output feedback stabilisation for a class of continuous-time dynamic systems under sample-data outputs. *International Journal of Control*, 84(8), 1408–1416.
- Tian, E., Yue, D., and Chen, P. (2008). Quantized output feedback control for networked control systems. *Information Sciences*, 178(12), 2734–2749.
- Wakaiki, M., Zama, T., and Liu, K.Z. (2017). Quantized output feedback stabilization by Luenberger observers. *IFAC-PapersOnLine*, 50(1), 2577–2582.
- Wang, X., Yu, H., and Hao, F. (2017). Observer-based disturbance rejection for linear systems by aperiodical sampling control. *IET Ctrl. Theory and Appl.*, 11(10), 1561–1570.